Volumetric measurements of a spatially growing dust acoustic wave

Jeremiah D. Williams

Citation: Phys. Plasmas **19**, 113701 (2012); doi: 10.1063/1.4766813
View online: http://dx.doi.org/10.1063/1.4766813
View Table of Contents: http://pop.aip.org/resource/1/PHPAEN/v19/i11
Published by the American Institute of Physics.

Volumetric measurements of a spatially growing dust acoustic wave

Jeremiah D. Williams[a)]
Physics Department, Wittenberg University, Springfield, Ohio 45504, USA

(Received 8 March 2012; accepted 25 October 2012; published online 13 November 2012)

In this study, tomographic particle image velocimetry (tomo-PIV) techniques are used to make volumetric measurements of the dust acoustic wave (DAW) in a weakly coupled dusty plasma system in an argon, dc glow discharge plasma. These tomo-PIV measurements provide the first instantaneous volumetric measurement of a naturally occurring propagating DAW. These measurements reveal over the measured volume that the measured wave mode propagates in all three spatial dimensional and exhibits the same spatial growth rate and wavelength in each spatial direction. © *2012 American Institute of Physics*. [http://dx.doi.org/10.1063/1.4766813]

I. INTRODUCTION

Dusty (complex) plasmas are four-component plasma systems that consist of ions, electrons, neutral particles, and charged microscopic particles or "dust." The dust, which typically consists of nanometer- to micrometer-sized particles in the laboratory environment, becomes charged through interactions with the background plasma. As a result, the dust component fully interacts with and self-consistently modifies the properties of the surrounding plasma medium. The presence of this third charged species results in a system that is significantly more complex than the traditional two-component plasma and supports a range of new plasma phenomena. Despite the increased complexity that this third charged species introduces, this system is experimentally attractive because the relatively large size and low charge state of the dust grains results in a system whose size and timescale allow the dust component to be studied at the kinetic level using diagnostic tools as simple as a video imaging. As a result, this field of study has seen a significant amount of growth and provided a great deal of insight into a wide range of basic physics over the past twenty years.

One consequence of the presence of this third charged species is that the plasma can support a number of new collective mode, including the dust acoustic wave (DAW). Since being initially predicted in 1990[1] and identified experimentally in 1995,[2] the DAW has been a topic of great experimental,[3–10] and theoretical,[11–14] interest within the dusty plasma community. While the majority of the experimental studies of this wave mode have been restricted to measurements in a two-dimensional plane (i.e., the slice of the dust cloud illuminated by a thin laser sheet) and a number of these studies have hinted that the wave motion associated the dust acoustic wave is three-dimensional, there have been relatively few studies that have examined the potential three-dimensional wave motion associated with this wave mode. Thomas and his collaborators have used stereo-particle image velocimetry (PIV) techniques[15] and laser light scattering (LLS) techniques to make measurements of the wave structure of a propagating dust acoustic wave. In particular, the stereo-PIV measurements[16,17] have suggested the possibility of wave motion in the transverse direction, which is in the direction perpendicular to the laser sheet used for illumination. However, diagnostic limitations prevented any definitive conclusions from being reached. In another study,[18] the laser sheet that illuminated a thin slice of the dust cloud was swept through the dust cloud in the direction perpendicular to the illumination sheet. Images at different spatial locations showed that the dust acoustic wave exhibited a three-dimensional structure that varied throughout the cloud volume. Menzel *et al.*[19] reported on measurements of the three-dimensional structure of the dust density wave under microgravity conditions. In this work, they used the observed spatial and temporal coherence of the wave mode in their experiment geometry and the assumption that the dust cloud geometry was rotationally symmetric to reconstructed the three dimensional structure of the wave mode by carefully correlating images taken using a scanning video microscopy system with a high speed camera, a process that is analogous to stroboscopic sampling. The reconstruction showed wave fronts that were concentrically arranged around the void. Finally, a later study by Heinenreich *et al.*[20] reported on observations of a propagating dust acoustic wave transitioning into a stationary dust density structure when the discharge current exceeded a threshold value. Once this stationary structure was present, they were able to measure that these standing structures were arranged in a nested conical structure by scanning a laser sheet through the cloud volume.

In this paper, the volumetric properties of a naturally occurring propagating dust acoustic wave are examined using diagnostic techniques previously unavailable to researchers in the field of dusty plasmas. In particular, a careful analysis of tomographic particle image velocimetry (tomo-PIV)[21] measurements is made to examine the properties of the naturally occurring, propagating dust acoustic wave over an *extended* volume. Specifically, we examine the three-dimensional motion of the particles associated with this wave mode and the distribution of velocities when the wave mode is present under a single set of experimental conditions by examining the three-dimensional velocity field that is measured using tomographic PIV techniques. From

[a)]Electronic mail: jwilliams@wittenberg.edu.

these velocity measurements, the wavelength and growth rate for the observed wave mode are found. To our knowledge, this is the first instantaneous measurement of a propagating dust acoustic wave that has been made over an extended volume. In Sec. II, the experimental setup and measurement methods are discussed. A discussion of the measurements can be found in Sec. III.

II. EXPERIMENTAL TECHNIQUES

The experimental measurements of the dust acoustic wave that are presented here were performed in the Wittenberg University DUsty Plasma DEvice (WUDUPE).[22] The WUDUPE is a dc discharge plasma device that is comprised of a t-shaped vacuum vessel having sides of 12″ and an inner diameter of 6″. A large rectangular viewport provides optical access for the tomo-PIV diagnostic. Argon plasmas are generated by biasing a 2.54 cm (1 in.) diameter brass electrode positive with respect to the grounded vacuum vessel chamber walls using a constant current high voltage supply. Here, an argon dc glow discharge was generated at a neutral gas pressure of 65 mTorr in the WUDUPE device by applying a 0.6 mA, 240 V dc signal to the electrode. A second electrically floating 2.54 cm brass electrode positioned approximately 5 cm below the biased electrode was loaded with 1.98 μm diameter melamine microspheres ($\rho = 1510\,\mathrm{kg/m^3}$) that served as the source powder for the clouds studied here. Under these conditions, a dust cloud containing a naturally occurring dust acoustic wave spontaneously forms below the anode in the anode spot of the discharge. A schematic drawing of the WUDUPE device and the tomo-PIV diagnostic is shown in Figure 1. A representative image of the dust cloud examined in this study is seen in Figure 2. Here, the wave structure is seen in the higher density region of the cloud indicated by arrows.

The microparticles in the dusty plasma are imaged using a four camera system operating at 15 Hz and then analyzed using particle image velocimetry techniques.[23] In the typical application of the PIV technique to dusty plasmas, a pair of short laser pulses (~10 ns in duration) follow the same optical path and are expanded to illuminate a thin slice of the dusty plasma system. The two laser pulses are separated in time by a user-

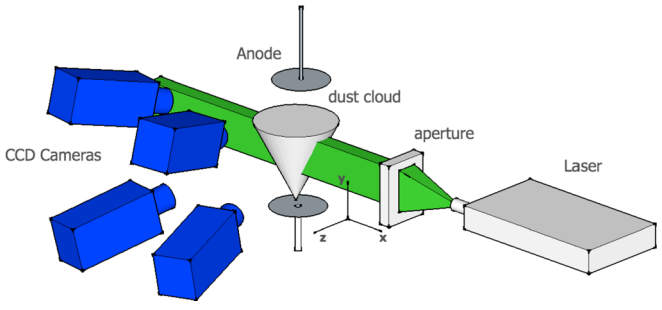

FIG. 1. Schematic of the WUDUPE device and the tomographic PIV diagnostic. The source dust for the experiments presented here is located on an electrically floating tray positioned approximately 5 cm below the anode, which is connected to a constant current, high voltage supply. A 3 mm thick volume of the dust cloud is illuminated using a laser and imaged using four cameras. The coordinate system shown in this figure is defined by the illumination volume and will be used throughout this text, with the –*y*-direction being defined by the direction of gravity.

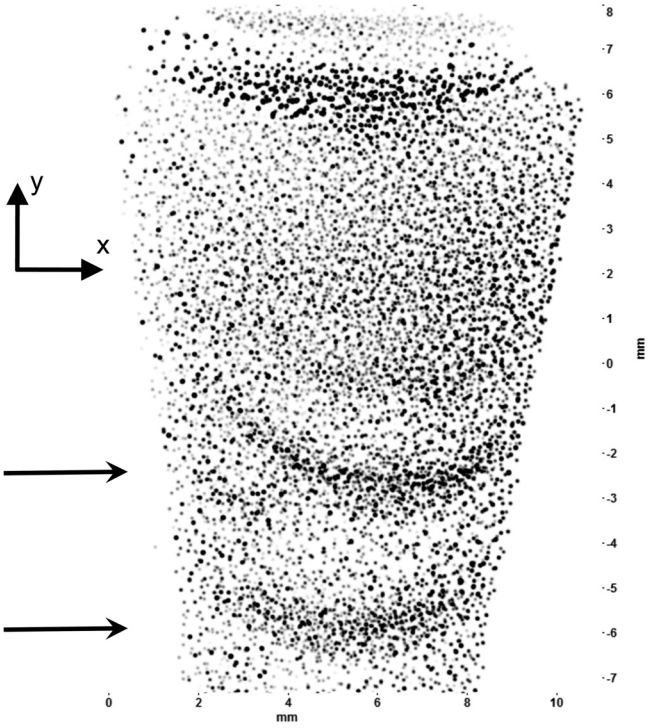

FIG. 2. A representative (inverted) photograph of the dust cloud examined in the experiments presented here. The arrows indicate the position of wave fronts of the dust acoustic wave that are visible in the optical data. It is noted that this image is one of the three images that are used to reconstruct one of the two illuminate volumes, represented as a 3D intensity field that the PIV analysis (3D cross correlation analysis) is performed on.

defined interval, typically $0.25 \leq \Delta t_{laser} \leq 30$ ms, which allows for studies of kinetic motion (smaller values of Δt_{laser}) or fluid motion (larger values of Δt_{laser}).[24] For the experiments presented here, $\Delta t_{laser} = 3$ ms. Depending on the PIV technique employed, the dust particles are then imaged by as many as four, typically charge coupled device (CCD), cameras which are synchronized to the laser pulses. The light from each laser pulse is recorded to separate video frames and the average motion of the particles in a sub region of the imaged cloud is found by performing a correlation analysis between similar sub regions in the images from each camera recorded during a laser pulse. Consequently, the PIV technique does not measure the motion of individual particles, as is the case in the particle tracking techniques that are often employed in dusty plasma experiments.[25] Instead, the PIV technique is a fluid measurement that provides information on the motion of clusters of particles. In the past, two-dimensional[26] and stereoscopic[15] techniques have been applied in experimental studies of the dust acoustic wave.[8,17,27] A key limitation in these studies was that they were restricted to measurements over a thin slice of the dust cloud.

In this study, 145 tomographic PIV (tomo-PIV) measurements[21] of the DAW were made. In the tomographic approach, a laser pulse is expanded using a combination of spherical and cylindrical lenses to illuminate a volume of the dust cloud, which is then typically imaged using four cameras. To improve the volumetric reconstruction, the illumination beam is clipped using a rectangular aperture to ensure that a rectangular volume of the dusty plasma is illuminated.

For the measurements presented here, a 3 mm thick slice of the dust cloud is illuminated. It is noted that the number density of the clouds examined here is sufficiently low that only three cameras are needed for tomographic reconstruction.[28]

The set of images taken by the three cameras during each laser pulse, one of which is seen in Figure 2, are then used to reconstruct the illuminated volume, creating a 3D intensity field using five iterations of the multiplicative algebraic reconstruction technique (MART)[29] over a $17 \times 15 \times 3$ mm^3 volume discretized with $957 \times 867 \times 226$ voxels. The reconstruction process was improved through the use of image preprocessing with background intensity removal, particle intensity equalization, and a Gaussian smoothing (3×3 kernel size). Each reconstructed intensity distribution is then decomposed into a series of $n \times p \times q$ voxel subregions (e.g., interrogation region) and the average displacement of the particles within each of these subregions is then found by performing a three-dimensional cross correlation analysis,[30] which produces a three dimensional, three-component (3D3C) velocity field over the measurement volume. The high magnification and the lower number densities resulted in the use of a large interrogation size of $n = p = q = 64$ for the measurements presented here; corresponding to an interrogation volume of $\sim$1 mm^3. Given the relatively large size of the interrogation volume, a 75% overlap of the interrogation regions was used to increase the spatial resolution.

III. MEASUREMENTS

To examine the instantaneous properties of the DAW, we focus our attention on a single, representative tomographic PIV measurement. It is noted that, unlike previously reported measurements of the DAW that have been made in the WUDUPE device,[22,31] the wave fronts of the naturally occurring DAWs that are examined here, Figure 2, exhibit significant curvature. From these images, we are able to estimate the wavelength and the phase speed of the wave. To find the wavelength, a $\sim$0.1 mm (8 pixel) wide vertical intensity profile from across the image are fit to a sinusoidal function over the entire measurement sequence. From these fits, we estimate the wavelength to be 3.21 ± 0.05 mm. The phase speed of the dust acoustic wave is found by tracking the position of the wave fronts between successive images. This resulted in a phase speed of 17.7 ± 1.2 mm/s. Since the measurement rate for the tomographic system was 15 Hz, it was not possible to directly measure the frequency of the measured dust acoustic wave. However, it is possible to estimate the frequency by assuming that the observed wave mode is linear and in the long wavelength limit ($k^2\lambda_D^2 \ll 1$) under typical laboratory condition ($T_i \ll T_e$). Under these conditions, this wave mode exhibits an acoustic dispersion relation,[1] which we use to estimate the frequency of the measured dust acoustic wave to be 5.5 ± 0.5 Hz. This result that is consistent with previous measurements in the WUDUPE device under similar experimental conditions. It is noted that, while the large amplitudes of the observed wave mode suggest that these waves are nonlinear, this approach has been used previously[17] to provide a reasonable estimate of the frequency of the wave mode. These measurements of the wavelength and phase speed will be compared to results estimated from the tomographic PIV measurements.

To obtain a measure of the instantaneous properties the wave mode, we use a characteristic feature of the DAW that has been observed in previous measurements;[17,27,32] namely, that bulk motion of the dust grains are correlated with the wave structure that is seen in the dust density perturbations of the wave. In particular, the velocity vectors associated with the particle motion in the wave front point in the direction of wave propagation, while velocity vectors associated with the particle motion on either side of the wave front point in the direction opposite of the wave propagation. As such, isosurfaces representing where the velocity is zero provides a measure of the structure in this wave mode. It is noted that while the direction of wave propagation is in a direction perpendicular to the wave front and that observed curvature of the wave front indicates that direction of the wave propagation does change across the wave front, it is observed that this characteristic feature is most pronounced in direction of the ion flow, here the y-direction based on the electrode configuration seen in Figure 1. This result is consistent with previous measurements and results in only the y-component of the velocity being zero across the entire wave front. As a result, isosurfaces representing where the y-component of the velocity is zero are used, Figure 3(a). It is noted that the use of isosurfaces at $v_y = 0$ results in the depiction of half wavelengths, since $v_y = 0$ occurs twice per wavelength. To examine what is happening in each vector component, we plot contours of the x-, y-, and z-component of the PIV velocities at three spatial locations representing the right ($x = 3.5$ mm), center ($x = 5.5$ mm), and left ($x = 7.5$ mm) sides of the wave front seen in Figure 2. These contours are plotted in Figures 3(b)–3(d), respectively. The appearance of the banded structure in the contour slices indicates that the wave structure is present in each spatial direction, though there does appear to be spatial dependence to the wave structure. It is observed that the wave structure is apparent in the x-component of the velocity only on the sides of the wave front where the curvature is greatest. By contrast, the wave structure is observed across the entire wave front in the y-component of the velocity and is observed to be most pronounced in the y-component of the velocity in the central region of the wave front, where there is relatively little curvature in the wave fronts. These two observations are consistent with what is seen in the images of the wave fronts, where the wave fronts are observed to propagate in a direction that is perpendicular to the wave fronts. Finally, it is observed that there is evidence of wave structure in the z-component of the velocity across the entire wave front, though it is not as pronounced as in the y-direction. This result is consistent with previous measurements,[17] where there was an indication that there might be transverse motion. It is particularly interesting to note that the particle motion associated with this wave mode does appear to be coupled. For example, a comparison of Figures 3(b) and 3(c) reveals that at the edges of the wave front (i.e., in the region where the curvature of the wave fronts is most pronounced),

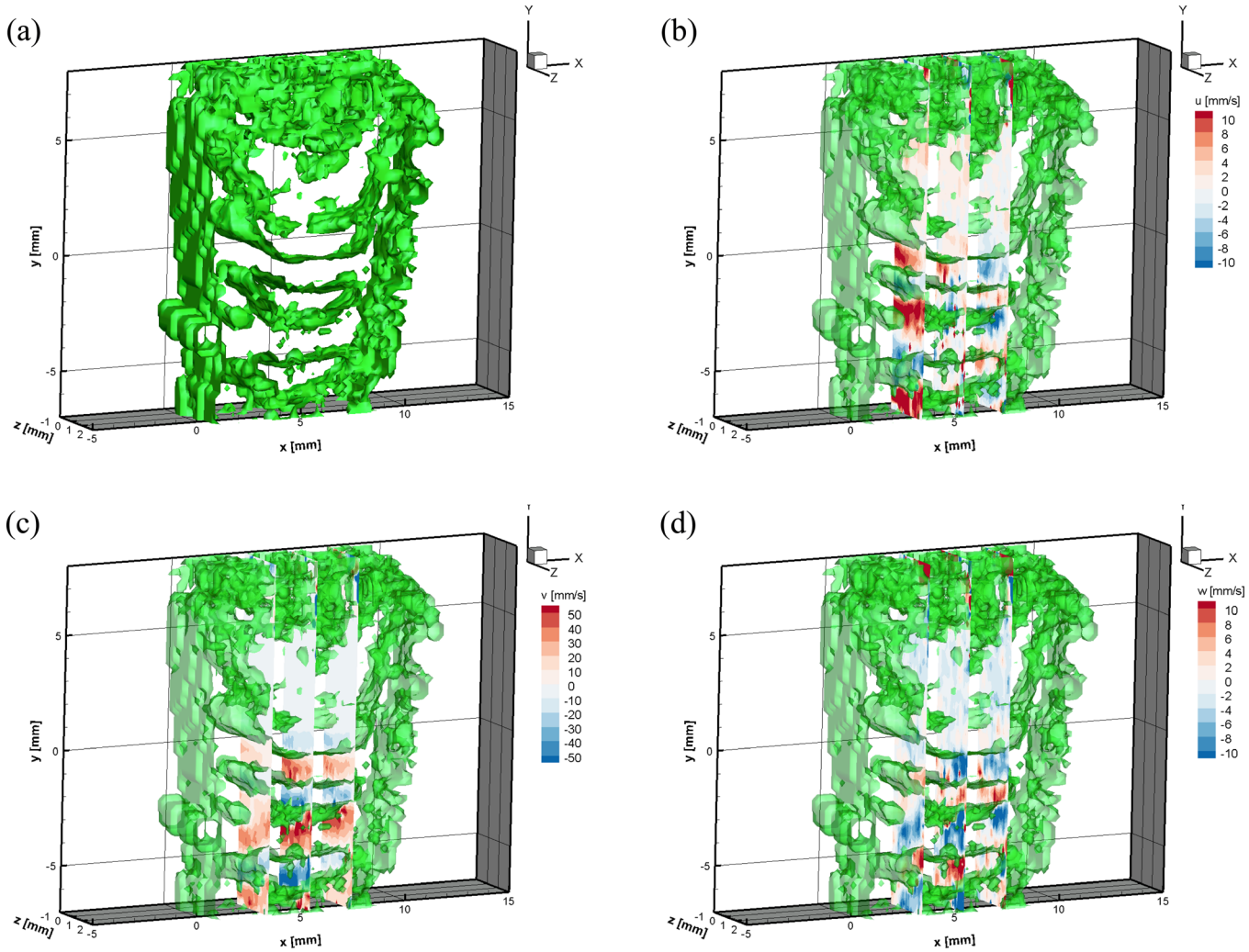

FIG. 3. A representative volumetric velocity field of the dust clouds examined here. The wave fronts are identified by plotting isosurfaces of $v_y = 0$ in (a), while the (b) x-, (c) y-, and (d) z-component of the velocity field at three spatial locations representing the right ($x = 3.5$ mm), center ($x = 5.5$ mm), and left ($x = 7.5$ mm) sides of the wave front are superimposed on the isosurfaces of $v_y = 0$. The bands that are seen in superimposed surfaces show that oscillations associated with the wave mode are present in each vector direction.

the motions in the x- and y-direction are coupled. In particular, the particles on the leading edge of the wave front are observed to moving up (i.e., in the $+y$-direction, opposite the direction of gravity) and toward the center of the cloud, while particles in the wave front are observed to moving down (i.e., in the -y-direction, in the direction of gravity) and away from the center of the cloud. A comparison of Figures 3(c) and 3(d) reveals that the motions in y- and z-direction are coupled across the wave front as well. In particular, the particles on the leading edge of the wave front are observed to be moving against the direction of gravity ($+y$-direction) and toward the back of the dust cloud (i.e., the $-z$-direction, toward the cameras), while in the wave front the particles are observed to be moving in the direction of gravity ($-y$-direction) and toward the front of the dust cloud ($+z$-direction). While this type of motion has been hinted at in previous measurements, this represents the first instantaneous measurement of this coupled motion and represents one of the advantages that the tomographic PIV approach provides. Further, the increased resolution of the measurements presented here and the volumetric information that is provided by the tomographic PIV approach suggests that it may be necessary to include transverse motion in the theoretical formalism of this wave mode.

To obtain a quantitative measure of the volumetric structure of this wave mode, a 0.5 mm thick vertical slice of the velocity field is extracted from a single z-plane of the tomographic measurement. A comparison of one such velocity profile in each spatial direction is seen in Figure 4. It is observed that the wave structure is observed in all three spatial components of the velocity of the dust grains, though the velocity of the dust grains is notably smaller in the x- and z- direction, and that the amplitude grows as wave propagates in the direction of decreasing y (i.e., the direction of ion flow and gravity). It is also observed that the wave structure is observed in the PIV vectors prior to being visible in the video images, a result that is consistent with previously made measurements using stereo-PIV techniques.[17]

To extract the measurements of the wavelength and the spatial growth rate, we assume that the wave mode exhibits exponential growth[17] and model the experimentally

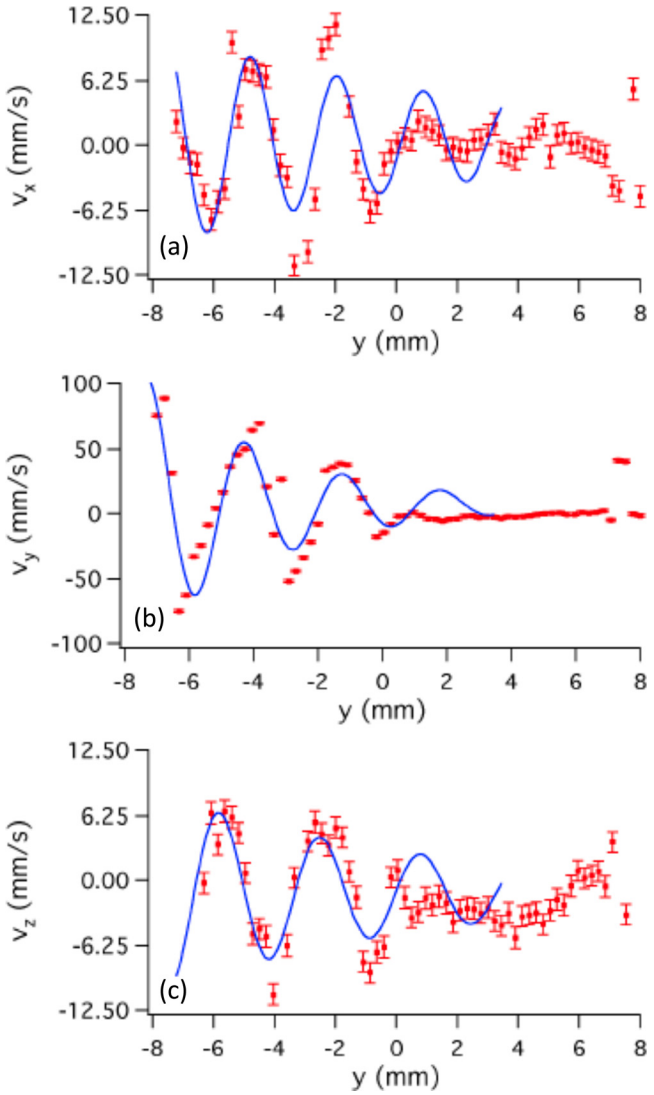

FIG. 4. Comparison between the experimentally measured velocity profile in the (a) x-, (y) y-, and (c) z-direction and the model of the spatially growing wave given by Eq. (1).

measured velocity structure in each spatial direction direction, j, using

$$v_j(y) = v_{\max,j} \exp(\gamma_j y) \cos\left(\frac{2\pi}{\lambda_j} y\right), \quad (1)$$

where $v_{max,j}$ is the peak particle speed in the j^{th} spatial direction, γ_j and λ_j are fit parameters that give us the growth rate and wavelength in the j^{th} vector direction. This fit is done over the entire volumetric measurement. The wavelengths and growth rates that are extracted from this fitting are seen in Figure 5. It is noted that, while the fits seen in Figure 4 are comparable to what has been seen previously,[17] the fits do not necessarily fit all of the data points. To address this, the fit parameters are then filtered to ensure that only those with small uncertainty are included in Figure 5. Here, the wavelength and growth rate in each spatial direction (Figures 5(a) and 5(d) depict the measured values in x-direction, Figures 5(b) and 5(e) in the y-direction and Figures 5(c) and 5(f) in the z-direction) are plotted as function of the location in the illuminated volume. The plots in Figure 5 depict the results from a single tomo-PIV measurement and each point in this plot represents a wavelength and growth rate extracted from the fits seen in Figure 4. The white regions in these figures indicate locations where the fit failed to find a reliable value for the wavelength or growth rate. It is observed that the wavelength and growth rate in each vector direction tends to be clustered in different regions of the illuminated volume of the cloud. This analysis reveals that the wave structure is present the x-direction in the regions of the cloud, Figure 2, where the curvature of the wave fronts is greatest. This result is consistent with what was observed in Figure 3(b), where contours of v_x showed evidence of wave motion only in the regions where the curvature of the wave fronts is greatest. By contrast, the wave structure is present throughout the cloud in the y- and z-direction. However, the wave structure is significantly more pronounced in the y-direction; a result that is also consistent with the contours of v_y and v_z that are seen in Figures 3(c) and 3(d), respectively. This may be a consequence of the experimental geometry and the resulting ion flow that drives the observed wave mode. These measurements, taken in combination with the motion that is seen in Figure 3, suggest that the wave motion associated with the dust acoustic wave is three dimensional.

To determine a representative wavelength and growth rate for each tomographic measurement, the average value for the wavelength and growth rate are computed using all of the wavelengths and growth rates that are seen in Figure 5. The wavelength and growth rate over the duration of the 145 tomo-PIV measurement sequence are seen in Figure 6. It is observed that the wavelength and growth rate are relatively constant over the duration of the measurement and the same in each vector direction. By taking the average of the values plotted in Figure 6, we compute a representative wavelength and growth rate in each vector direction for the wave mode examined here. We were also able to measure the speed of the wave in each vector direction by tracking a peak in the fit of the wave structure. From the phase speed, c_{da}, and the wavelength, the frequency of the wave mode, f_{da}, is calculated under the assumption of a linear mode and typical laboratory conditions, $T_i \ll T_e$. These results are summarized in Table I. It is noted that the measurement of the wave properties are consistent in each vector direction, suggesting that the overall wave properties that are observed are similar in each spatial dimension in spite of the significant spatial variation that is observed, and that the results obtained using tomographic PIV measurements are consistent with the optical measurements. The consistency in each spatial direction for the wavelength and growth rate suggest the possibility of a rotational symmetry in the observed wave mode with respect to the direction of ion flow (i.e., the y-direction), a results that is consistent with measurements by Menzel *et al.*[19] However, the growth rate found here is notably smaller than results reported by Thomas,[17] who measured the growth rate by applying the procedure used here to stereoscopic PIV data. However, in that paper, the experiments were performed using notably large particles (a nominal diameter of 30 μm compared to 1.98 μm diameter particles used here) and at higher neutral gas pressures. These differences will be examined more closely in a future work.

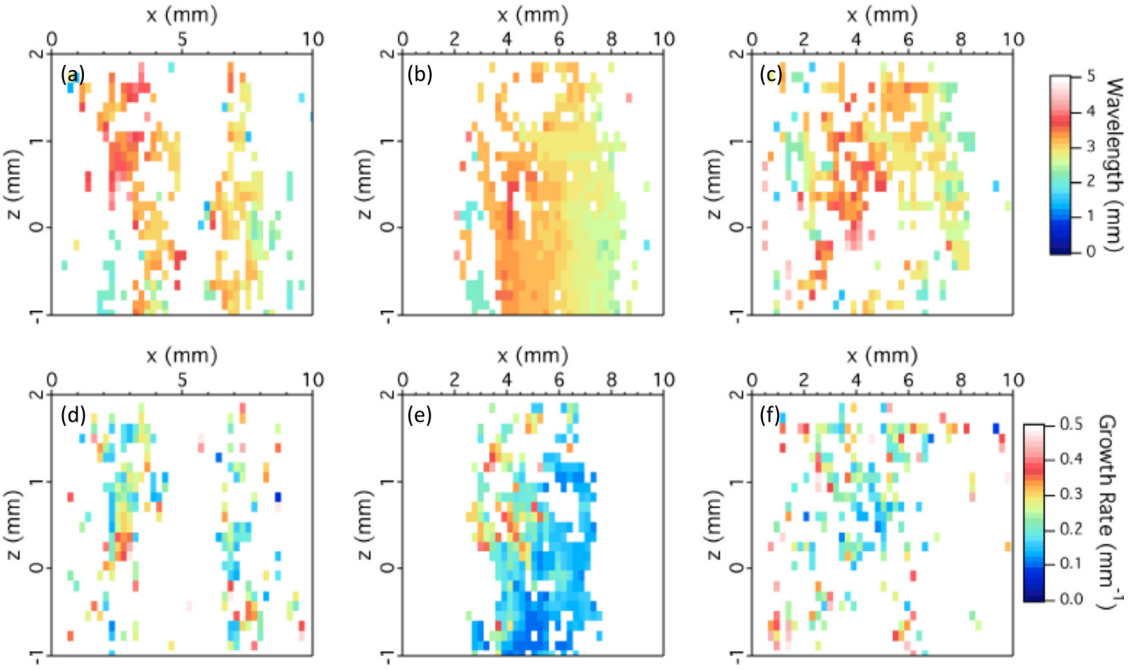

FIG. 5. Plot of the (a) wavelength and (b) growth rate of the wave mode from a single tomo-PIV measurement in each vector direction over the measurement volume. Each point in this plot represents a wavelength and growth rate extracted from the fit seen in Figure 4. It is noted that oscillations are present throughout the measurement volume in the *y*- and *z*-direction, while it is localized on the sides of the wave where the curvature is greatest in the *x*-direction.

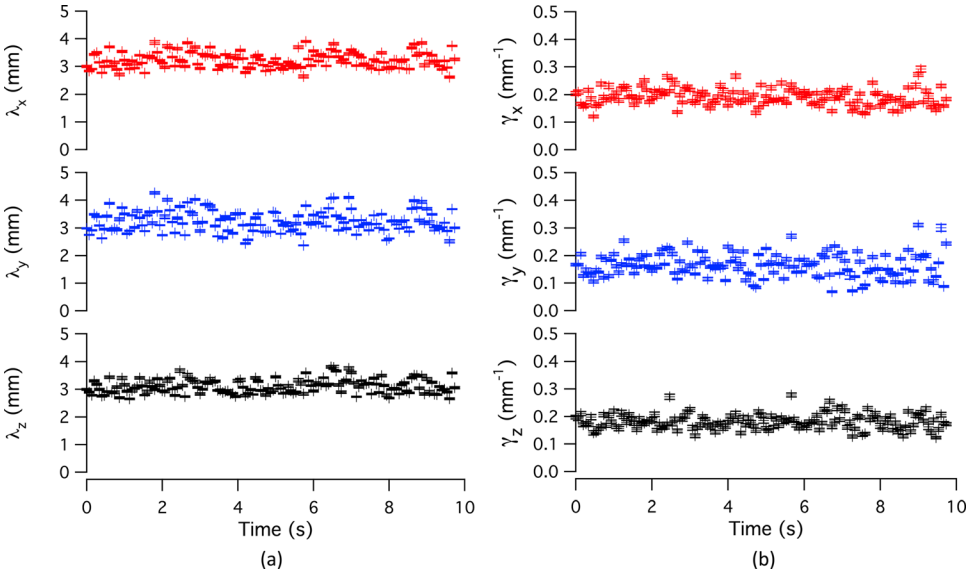

FIG. 6. Plot of the (a) wavelength and (b) growth rate in each vector direction over the measurement sequence. It is observed that the wavelength and growth rate are relatively constant over the measurement duration and similar in each vector direction.

Finally, since each tomo-PIV measurement results in over 70 000 three-dimensional velocity measurements over the illuminated volume of the dust cloud, we are able to construct distributions of velocities for each measurement made. A representative distribution of measured velocities in each vector direction over the illuminated measurement volume from a single tomo-PIV measurement is seen in Figure 7(a). It is observed that the distributions in *x*- and *z*-direction appear symmetric, while the velocities in the *y*-direction (the direction in which the wave propagation is most pronounced) appear to be highly asymmetric. To get a better sense of the measured distributions and to determine if this asymmetry is a consequence of the wave mode, we construct distributions of velocities from the upper ($y \geq 1$ mm) and lower ($y < 1$ mm) regions of the cloud, Figures 7(b) and 7(c) respectively. It is noted that, based on the PIV data, there is some evidence of very small amplitude waves in the upper region, while the wave mode is the dominant feature in the lower region of the cloud. It is observed that in the upper

TABLE I. Summary of experimental measurements of the wave properties.

Data source	λ (mm)	γ (mm^{-1})	c_{da} (mm/s)	f_{da} (Hz)
v_x	3.2 ± 0.4	0.12 ± 0.04	14.8 ± 2.2	4.6 ± 1.1
v_y	3.2 ± 0.4	0.11 ± 0.05	17.0 ± 1.8	5.3 ± 1.2
v_z	3.1 ± 0.3	0.08 ± 0.03	15.3 ± 3.2	4.9 ± 1.4
Image	3.2 ± 0.1		17.6 ± 1.2	5.5 ± 0.5

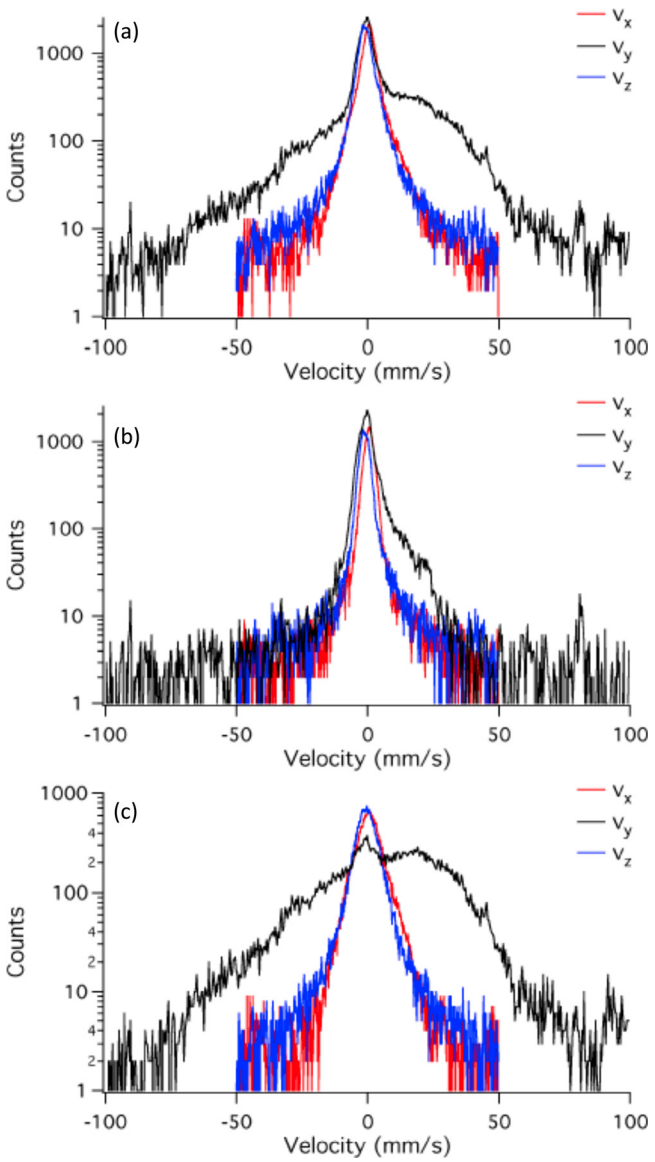

FIG. 7. (a) Plot of the distribution of velocities from a single tomo-PIV measurement over the entire measurement volume. Histograms of a two-dimensional velocity subspace from the upper region ($y > 1$ mm) and lower regions ($y < 1$ mm) of the measurement volume are seen in (b) and (c), respectively.

region of cloud, the distribution of velocities in each vector direction is reasonably symmetric. By contrast, the measured distribution of velocities shows significant spreading in the lower region of the cloud and a very pronounced asymmetry, particularly in the *y*-direction. As a result, we attribute the observed asymmetry to the existence of the wave mode. This will be examined in more detail in a future paper.

IV. SUMMARY

To summarize, this paper describes the use of the tomographic PIV technique to provide the first instantaneous, volumetric measurement of the properties of a propagating dust acoustic wave. It is observed that the wave structure is present in all three spatial dimensions but that the motion associated with the wave mode exhibits significant spatial dependence. It is also observed that the wave properties (wavelength, growth rates, wave speed) are comparable in each spatial direction, suggesting that the measured wave exhibits a rotational symmetry about the direction of ion flow based on the experimental geometry. It was also observed that the distribution of velocities associated with the wave motion exhibits a large anisotropy, particularly in the direction of ion flow.

ACKNOWLEDGMENTS

This work was supported by National Science Foundation Grant No. PHY-0953595.

[1]N. Rao, P. K. Shukla, and M. Y. Yu, Planet. Space Sci. **38**, 543 (1990).
[2]A. Barkan, R. L. Merlino, and N. D'Angelo, Phys. Plasmas **2**, 3563 (1995).
[3]V. E. Fortov, O. F. Petrov, V. I. Molotkov, M. Y. Poustylnik, V. M. Torchinsky, A. G. Khrapak, and A. V. Chernyshev, Phys. Rev. E **69**, 016402 (2004).
[4]M. Schwabe, M. Rubin-Zuzic, S. Zhdanov, H. M. Thomas, and G. E. Morfill, Phys. Rev. Lett. **99**, 095002 (2007).
[5]J. D. Williams, E. Thomas, Jr., and L. Marcus, Phys. Plasmas **15**, 043704 (2008).
[6]I. Pilch, T. Reichstein, and A. Piel, Phys. Plasmas **16**, 123709 (2009).
[7]V. Nosenko, S. K. Zhdanov, S.-H. Kim, J. Heinrich, R. L. Merlino, and G. E. Morfill, EPL **88**, 65001 (2009).
[8]E. Thomas, Jr., Phys. Plasmas **17**, 043701 (2010).
[9]T. M. Flanagan and J. Goree, Phys. Plasmas **17**, 123702 (2010).
[10]J. R. Heinrich, S.-H. Kim, J. K. Meyer, and R. L. Merlino, Phys. Plasmas **18**, 113706 (2011).
[11]M. Rosenberg, J. Plasma Phys. **67**, 235 (2002).
[12]M. Rosenberg, E. Thomas, Jr., and R. L. Merlino, Phys. Plasmas **15**, 073701 (2008).
[13]K. Avinash, R. L. Merlino, P.K. Shukla, Phys. Lett. A **375**, 2854 (2011).
[14]V. V. Yaroshenko *et al.*, Phys. Plasmas **19**, 023702 (2012).
[15]E. Thomas Jr., J. D. Williams, and J. Silver, Phys. Plasmas **11**, L37 (2004).
[16]E. Thomas, Jr. and J. Williams, Phys. Plasmas **13**, 055702 (2006).
[17]E. Thomas, Jr., Phys. Plasmas **13**, 042107 (2006).
[18]E. Thomas, Contrib. Plasma Phys. **49**, 316 (2009).
[19]K. O. Menzel, O. Arp, D. Caliebe, and A. Piel, IEEE Trans. Plasma Sci. **38**, 838 (2010).
[20]J. R. Heinrich, S.-H. Kim, and R. L. Merlino, Phys. Rev. E **84**, 026403 (2011).
[21]J. D. Williams, Phys. Plasmas **18**, 050702 (2011).
[22]J. D. Williams and J. Duff, Phys. Plasmas **17**, 033702 (2010).
[23]M. Raffel, C. Willert, and J. Kompenhans, *Particle Image Velocimetry: A Practical Guide*, 2nd ed. (Springer, 2007).
[24]J. D. Williams and E. Thomas, Phys. Plasmas **14**, 063702 (2007).
[25]Y. Feng, J. Goree, and B. Liu, Rev. Sci. Instrum. **78**, 053704 (2007).
[26]E. Thomas, Jr., Phys. Plasmas **6**, 2672 (1999).
[27]E. Thomas, Jr., IEEE Trans. Plasma Sci. **30**, 88 (2002).
[28]J. Williams, "Measurement of the three-dimensional wave process in the dust acoustic wave," Bull. Am. Phys. Soc. **56**, CP9.42 (2011).
[29]G. E. Elsinga, F. Scarano, B. Wieneke, and B. W. van Oudheusden, Exp. Fluids **41**, 933 (2006).
[30]G. E. Elsinga, B. Wieneke, F. Scarano, and A. Schröder, in *Particle Image Velocimetry New Developments and Recent Applications*, edited by A. Schroeder and C. Willert (Springer, Berlin, 2008), Topics in Applied Physics, Vol. 112, pp. 103.
[31]J. Williams and E. Snipes, IEEE Trans. Plasma Sci. **38**, 847 (2010).
[32]C.-T. Liao, L.-W. Teng, C.-Y. Tsai, C.-W. Io, and I. Lin, Phys. Rev. Lett. **100**, 185004 (2008).